JOURNAL OF MAGNETIC RESONANCE **132,** 191–196 (1998)
ARTICLE NO. MN981416

^{13}C-NOESY-HSQC with Split Carbon Evolution for Increased Resolution with Uniformly Labeled Proteins

Matthias Baur, Gerd Gemmecker, and Horst Kessler

Institut für Organische Chemie und Biochemie, Technische Universität München, Lichtenbergstrasse 4, D-85747 Garching, Germany

Received August 29, 1997; revised February 6, 1998

Two new pulse sequences are presented for the recording of 2D ^{13}C-HSQC and 3D ^{13}C-NOESY-HSQC experiments, containing two consecutive carbon evolution periods. The two periods are separated by a *z*-filter which creates a clean C_xH_z-quantum state for evolution in the second period. Each period is incremented (in a *non*-constant-time fashion) only to the extent that the defocusing of carbon inphase magnetization through *J*-coupling with neighboring carbons remains insignificant. Therefore, ^{13}C homonuclear *J*-couplings are rendered ineffective, reducing the loss of signal and peak splitting commonly associated with long ^{13}C evolution times. The two periods are incremented according to a special acquisition protocol employing a ^{13}C–^{13}C gradient echo to yield a data set analogous to one obtained by evolution over the added duration of both periods. The spectra recorded with the new technique on uniformly ^{13}C-labeled proteins at twice the evolution time of the standard ^{13}C-HSQC experiment display a nearly twofold enhancement of resolution in the carbon domain, while maintaining a good sensitivity even in the case of large proteins. Applied to the IIA^{Man} protein of *E. coli* (31 kDa), the ^{13}C-HSQC experiment recorded with a carbon evolution time of 2 × 8 ms showed a 36% decrease in linewidths compared to the standard ^{13}C-HSQC experiment, and the *S*/*N* ratio of representative cross-peaks was reduced to 40%. This reduction reflects mostly the typical loss of intensity observed when recording with an increased resolution. The ^{13}C-NOESY-HSQC experiment derived from the ^{13}C-HSQC experiment yielded additional NOE restraints between resonances which previously had been unresolved. © 1998 Academic Press

Key Words: **^{13}C-NOESY-HSQC; uniformly ^{13}C-labeled proteins; split evolution time; enhanced resolution; C–C gradient echo.**

INTRODUCTION

The determination of the structure of biopolymers by NMR relies to a large part on NOE-derived proton–proton distances obtained from multi-dimensional NOE spectroscopy (*1–5*). In proteins the NOE-derived distances between protons of different side chains constitute the essential experimental information to determine the 3D structure. These NOE distances are usually evaluated from carbon-edited NOESY spectra of uniformly ^{13}C-labeled proteins. However, these spectra often display severe overlap between signals. Here we present new experiments to record ^{13}C-HSQC and ^{13}C-NOESY-HSQC spectra with a split carbon evolution period, allowing the incrementation of the carbon magnetization to twice the standard duration on uniformly ^{13}C-labeled proteins. This results in a twofold enhancement in resolution and a significant reduction of signal overlap. At the same time the experiments display high signal intensity even in the case of large proteins.

Difficulties in achieving sufficient resolution in the carbon domain of NOESY spectra of uniformly ^{13}C-labeled proteins stem from scalar coupling of the carbons with neighboring carbons. To avoid substantial loss of signal and peak splitting due to the modulation of the inphase magnetization by the $^1J(^{13}C, ^{13}C)$ couplings (≈36 Hz), carbon evolution periods are usually limited to ca. 10 ms (*6*). Consequently, many cross-peaks are not separated in the carbon domain. To improve resolution, constant time evolution has to be used with an evolution period of 28 ms to refocus ^{13}C–^{13}C antiphase magnetization (*7, 8*). This approach leads to the separation of nearly all cross-peaks for typical proteins, even eliminating line broadening from spin–spin relaxation. However, in large nondeuterated proteins the resulting cross-peak intensities are very low. Moreover, the intensities also depend strongly on the spin–spin relaxation rate of the individual carbons, and it is therefore necessary to rescale the intensities of the NOE signals depending on their ^{13}C trace. In contrast, highly deuterated samples allow the use of constant time evolution of carbons while maintaining a good sensitivity (*9*). However, they in turn do not yield satisfactory NOE signals between aliphatic protons because of the low density of these protons (*10*).

Since none of the published techniques yields adequate resolution in the carbon domain combined with good sensitivity when applied to uniformly ^{13}C-labeled proteins, we have developed a modified 2D ^{13}C-HSQC experiment and the derived 3D ^{13}C-NOESY-HSQC experiment. In these the carbon magnetization evolves in two separate evolution periods. Each period is incremented (in a *non*-constant-time fashion) only to the extent that the defocusing of carbon inphase magnetization through *J*-coupling

1090-7807/98 $25.00

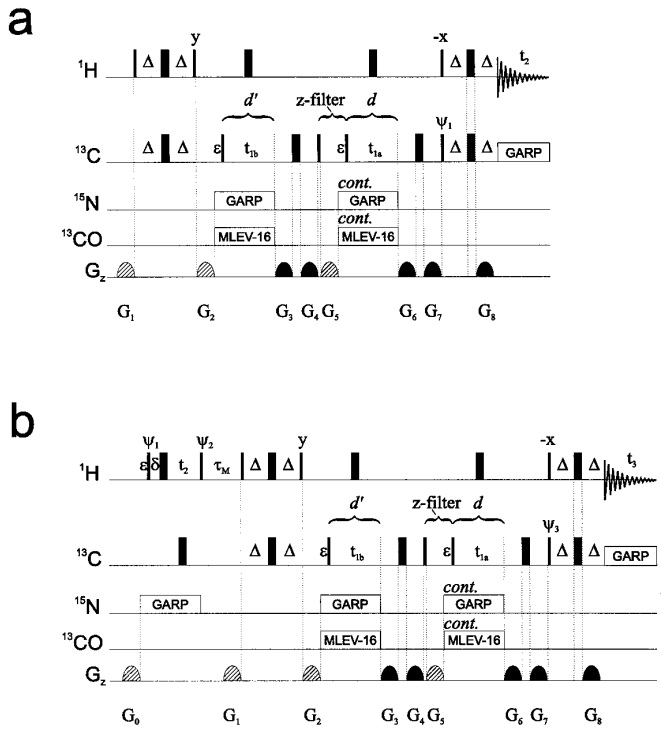

FIG. 1. 2D ^{13}C-HSQC (a) and 3D ^{13}C-NOESY-HSQC (b) experiments modified for split carbon evolution. Both experiments preserve the water magnetization at equilibrium and were applied to the IIA^{Man} protein. (a) ^{13}C-HSQC: The data set was recorded in two measurements corresponding to the two blocks of ^{13}C evolution. The same pulse program but different pulsed field gradient (PFG) strengths were used for each block of the experiment. The phase cycling during either block was $\psi_1 = x, -x$; *Rec* $= x, -x$. During the first block two scans were accumulated, during the second block, eight. (Also see general parameters below.) *First block:* The delay d was incremented starting at zero length (delay $d' = 0$). Quadrature detection was performed in STATES-echo–antiecho mode (*13, 21*), incrementing phase ψ_1 and inverting PFG G_8 for echo–antiecho selection. PFG strengths were $G_1 = 4\%$, $G_2 = 80\%$, $G_3 = 6\%$, $G_4 = 6\%$, $G_5 = 68\%$, $G_6 = 51.7\%$, $G_7 = -51.7\%$, and $G_8 = 26\%$. *Second block:* The delay d' was incremented starting at zero length for the first point. The delay d remained fixed at its maximal duration $N\Delta t_1$, where N is the number of *complex* carbon data points recorded during the first block and Δt_1 is the STATES-time increment. As above, quadrature detection was performed in STATES-echo–antiecho mode, incrementing phase ψ_1 and inverting PFG G_8 for echo–antiecho selection. PFG strengths were set to $G_1 = 4\%$, $G_2 = 80\%$, $G_3 = 10\%$, $G_4 = -10\%$, $G_5 = 80\%$, $G_6 = 41.7\%$, $G_7 = -41.7\%$, and $G_8 = 26\%$. (b) ^{13}C-NOESY-HSQC: Analogous to the ^{13}C-HSQC, the data set (domains $^{13}C(t_1) \times {}^1H(t_2) \times {}^1H^C$(Acq)) was collected in two measurements corresponding to the two blocks of incrementation of the $^{13}C(t_1)$ domain. The same pulse program, but different PFG strengths were used for each block of the experiment. The phase cycling during either block was $\psi_1 = x$; $\psi_2 = 45, -45$; $\psi_3 = 2x, 2(-x)$; *Rec* $= x, -x, -x, x$. Four scans (first block) and 16 scans (second block) were accumulated. Within each block the indirect $^1H(t_2)$ domain was recorded, interleaved with the $^{13}C(t_1)$ domain, as described in the following. First the evolution of the $^1H(t_2)$ domain was acquired according to the STATES-TPPI protocol (*21*), incrementing ψ_1 and *Rec*. However, following every $^1H(t_2)$ FID, the same FID was rerecorded with an inverted PFG G_8. Since inversion of the PFG G_8 selects the echo and antiecho signals for $^{13}C(t_1)$ evolution, this handling resulted in an interleaving of the $^{13}C(t_1)$ and the $^1H(t_2)$ domains. After completion of the incrementation in $^1H(t_2)$, the $^1H(t_2)$ evolution delay was reset to zero, the $^{13}C(t_1)$ evolution delay was incremented (by a STATES-time increment), and the procedure was restarted. Delays d and d' were used, analogous to the ^{13}C-HSQC for carbon incrementation. The resulting ^{13}C data set is analogous to one obtained by a STATES-echo–antiecho protocol. PFG strengths during the first block were $G_0 = 4\%$, $G_1 = 90\%$, $G_2 = 80\%$, $G_3 = 5\%$, $G_4 = 5\%$, $G_5 = 70\%$, $G_6 = 51.7\%$, $G_7 = -51.7\%$, and $G_8 = 26\%$. PFG strengths during the second block were $G_0 = 4\%$, $G_1 = 90\%$, $G_2 = 80\%$, $G_3 = 10\%$, $G_4 = -10\%$, $G_5 = 80\%$, $G_6 = 41.7\%$, $G_7 = -41.7\%$, and $G_8 = 26\%$. *General parameters:* Pulses, where no explicit phase is given, were applied along the x axis. PFGs had a sine-bell shape with a duration of 0.5 ms, followed by a 0.25-ms recovery delay. A PFG strength of 100% equals ca. 70 G/cm. Delays were $\Delta = 1.6$ ms, $\epsilon = 2.0$ ms, $\delta =$ length of 180° ^{13}C-pulse, $\tau_M = 130$ ms. The recycle delay was 1.3 s. RF power was 25 kHz (^{1}H) and 25 kHz (^{13}C). Decoupling denoted *cont.* was started where the previous decoupling had left off. For decoupling of ^{13}C a GARP train (*22*) (RF power 2.6 kHz), for ^{15}N a GARP train (*22*) (RF power 1.25 kHz), and for ^{13}CO a MLEV-16 train (*24*) of Gaussian inversion pulses of 800-μs length were used.

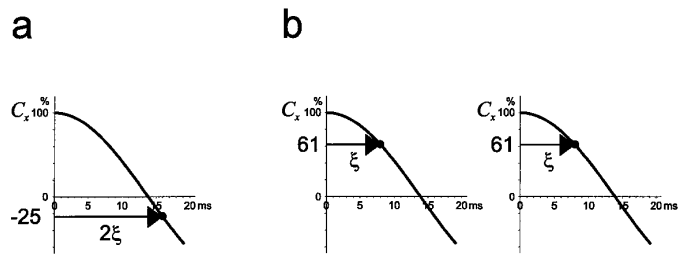

FIG. 2. Suppressing ^{13}C homonuclear J-couplings by dividing the evolution period into two parts: Evolving carbon magnetization to 16 ms (2ξ) results in signal loss and peak splitting due to the cosine modulation of the intensity of the transverse magnetization (C_xH_z) by $^1J(^{13}C, ^{13}C)$ couplings (a, where the effect of a single coupling is shown). In contrast, evolving the magnetization in two separate periods of 8 ms (ξ) each and ''combining'' the information from both periods to a data set analogous to one gained by evolution over the added time of both periods results in a line that is only slightly affected by ^{13}C–^{13}C J-couplings (b). This ''combination'' of information can be achieved by a ^{13}C–^{13}C gradient echo that relays information on the phase of magnetization from one period to the other and generates a joint signal.

with neighboring carbons remains tolerable. The information from the two periods is combined to give a data set corresponding to the evolution of the ^{13}C spins over the added duration of both periods. This is achieved by the use of a $^{13}C,^{13}C$ gradient echo (*11*) for part of the evolution time. This new technique effectively suppresses ^{13}C homonuclear J-couplings, thus eliminating loss of signal and peak splitting commonly associated with long ^{13}C evolution times. The spectra recorded with this technique, where the duration of each of the two periods is equal to the typical ^{13}C evolution time of the standard ^{13}C-HSQC experiment, display very good intensities even in the case of large proteins. The technique can also be adapted to a variety of problems by concatenating any number of these periods.

EXPERIMENTAL

Figure 1 shows the new ^{13}C-HSQC (Fig. 1a) and the derived ^{13}C-NOESY-HSQC (Fig. 1b) sequences. The pathway of mag-

netization through the ^{13}C-HSQC sequence starts out with excitation of proton coherence. Next, this magnetization is transferred to the directly bound carbon by the first 90° carbon pulse. In the subsequent period d' the magnetization is transverse on the carbon, before being converted to z-magnetization by the first 90° pulse of the central z-filter. The second 90° pulse of the z-filter returns the magnetization to the x, y-plane, and after completion of period d the magnetization is transferred back to the proton, where it is detected.

$$
\begin{aligned}
&-C_y \xrightarrow{\Omega_C t_{1b} C_z} -C_y\cos(\Omega_C t_{1b}) + C_x\sin(\Omega_C t_{1b}) \xrightarrow{G_3, 180_x, G_4} C_y\cos(\Omega_C t_{1b} + \varphi_{coil}(z)) + C_x\sin(\Omega_C t_{1b} + \varphi_{coil}(z)) \xrightarrow{90_x} \\
&C_z\cos(\Omega_C t_{1b} + \varphi_{coil}(z)) \xrightarrow{90_x} -C_y\cos(\Omega_C t_{1b} + \varphi_{coil}(z)) \xrightarrow{\Omega_C t_{1a} C_z} \cos(\Omega_C t_{1b} + \varphi_{coil}(z))\{-C_y\cos(\Omega_C t_{1a}) \\
&+ C_x\sin(\Omega_C t_{1a})\} \xrightarrow{G_6, 180_x, G_7} (1/2)\{C_y\cos(\Omega_C(t_{1b} + t_{1a})) + C_x\sin(\Omega_C(t_{1b} + t_{1a}))\}, \qquad [1]
\end{aligned}
$$

The ^{13}C-HSQC experiment is based on two main concepts. *First*, two separate periods are used, each of which is below the time required for the build-up of significant ^{13}C–^{13}C antiphase magnetization, thus suppressing ^{13}C homonuclear J-couplings (Fig. 2). The two evolution periods are consecutive with an intervening z-filter. This z-filter destroys the ^{13}C–^{13}C antiphase magnetization that has built-up during the first period d', creating a clean C_xH_z-quantum state for evolution in the second period d. *Second*, the two periods are incremented according to a protocol which results in a data set corresponding to evolution over the combined time of both periods, and which employs a ^{13}C–^{13}C gradient echo for part of the evolution time (Fig. 3). In this protocol both periods start out at zero length (the 180° proton pulses are neglected in the following). During the first phase of ^{13}C evolution the period d is incremented, while period d' remains at zero length (*first block*). During this block of the experiment the pulsed field gradients (PFG) G_1, G_2, and G_5 serve as spoil gradients, PFGs G_3 and G_4 cleanse the intervening 180° pulse (*12*), and PFGs G_6, G_7, and G_8 select the echo and antiecho signals for quadrature detection (*13*). After period d has been incremented to its maximum (ca. 8 ms), it is kept at this value and period d' is incremented (*second block*). The pulsed field gradients are now set to new values. PFGs G_1, G_2, and G_5 still serve as spoil gradients, but PFGs G_3, G_4, G_6, and G_7 now produce a ^{13}C–^{13}C gradient echo. This echo is set up so that the phase of the transverse magnetization hit by PFGs G_6 and G_7 is shifted by an amount corresponding to the evolution during d' ($=\Omega_C t_{1b}$ for any given carbon of resonance frequency Ω_C in the rotating frame). Thus, a signal arises at the end of period d that represents evolution over the combined time of the two periods. The ^{13}C–^{13}C gradient echo works analogously to the ^{1}H–^{1}H gradient echo used, for example, in the stimulated echo (*14*), the GOESY (*15*, *16*), and the diagonal-free NOESY (*17*) experiments. Using the product operator formalism in the Cartesian basis, the transfer of magnetization starting at the first 90° carbon pulse can be described as follows (only the desired magnetization is listed, $J(^{13}\text{C}, ^{13}\text{C})$ couplings are neglected):

where $\varphi_{coil}(z)$ denotes the phase shift created by PFGs G_3 and G_4 when twisting the transverse magnetization into a coil along the z-axis. As stated earlier, the last term corresponds exactly to evolution over the combined time of both periods. In addition to their role in the ^{13}C–^{13}C gradient echo, PFGs G_6 and G_7 together with PFG G_8 select the echo and antiecho components of the combined signal for quadrature detection. Because of the ^{13}C–^{13}C gradient echo, the sensitivity during the second block of incrementation is lowered to half its value during the first block (*11*). This reduced sensitivity is compensated for by accumulating four times as many scans during the second block of the experiment.

The ^{13}C-NOESY-HSQC (Fig. 1b) experiment has been derived from the ^{13}C-HSQC experiment by inserting a proton

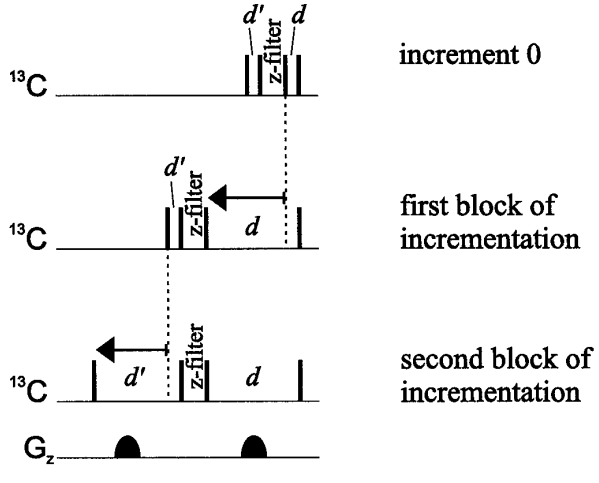

FIG. 3. Scheme of ^{13}C evolution. *No* constant time incrementation was performed. During the first block period d is incremented. During the second block period d' is incremented, while period d is kept at full extension. During this time PFGs produce a ^{13}C–^{13}C gradient echo to generate a signal corresponding to evolution over the combined time of both periods.

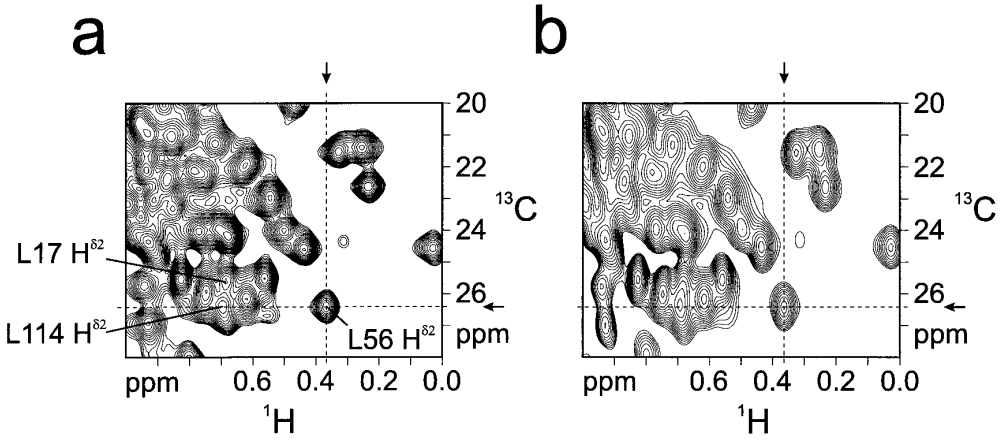

FIG. 4. Comparison of the ^{13}C-HSQC experiment (Fig. 1a) (a) and the standard ^{13}C-HSQC experiment (*20*) (b) recorded on IIA^{Man}. New high-resolution experiment (a): Both carbon periods were incremented to 7.9 ms, recording a total of 320 × 1024 real points (domains $^{13}C(t_1) \times {}^{1}H(Acq)$) with spectral widths of 10,000 Hz × 8333 Hz. The differences in intensities between the FIDs from the first and the second block were compensated for by dividing the amplitude of the FIDs from the second block by two before processing. Standard experiment (b): The carbon period was incremented to 7.9 ms, recording 160 × 1024 real points (domains $^{13}C(t_1) \times {}^{1}H(Acq)$) with spectral widths of 10,000 Hz × 8333 Hz. Both data sets were processed [in echo–antiecho manner (*13*)] to matrices of 512 × 2048 real points after apodization with a 90° shifted sine-bell window function and subsequent zero filling in both dimensions.

evolution period and NOE mixing time in front of the sequence, while keeping to the modified protocol for carbon recording. The suggested NOESY experiment preserves the water magnetization at equilibrium, ensuring an enhancement of the intensity of cross-peaks involving amide protons.

RESULTS

The new experiments were applied to a 31-kDa protein, the homodimeric IIA^{Man} domain of the mannose transporter of *E. coli* (*18*, *19*). The spectra were recorded at 310 K on a Bruker DMX600 spectrometer. A [U-^{15}N/^{13}C] sample was used with a concentration of about 0.8 mM (dimer) in 90% H_2O/10% D_2O and 10 mM Na-(P_i) buffer at pH 7.5. The symmetric IIA^{Man} dimer exhibits a single set of NMR signals, corresponding to the 135 amino acids of the monomer.

In a first step the parameters for the ^{13}C-HSQC experiment were optimized. Optimal sizes for the maximal evolution times in periods *d* and *d′* were obtained by recording the first block of incrementation (evolution time 16 ms) of a trial ^{13}C-HSQC on the IIA^{Man} protein. The data matrix was processed only in the acquisition domain, and 1D slices along t_1 were extracted from this interferogram at the position of signals which were resolved in the processed ^{1}H domain. These slices represent carbon FIDs. The time (t = 8 ms) at which the decay of the signals in these FIDs due to spin–spin relaxation (exponential decay) was as fast, that is, had the same derivative, as the decay due to the $^{1}J(^{13}C,$

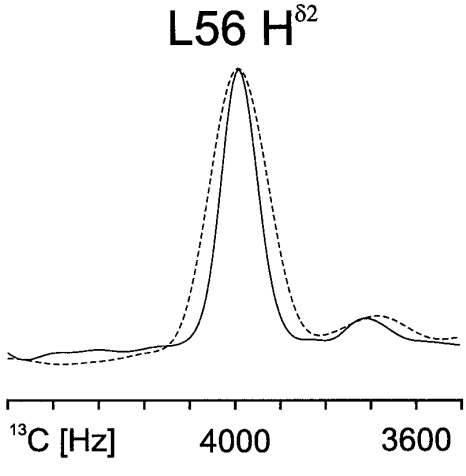

FIG. 5. 1D columns extracted from the 2D spectra of Fig. 4a (solid line) and Fig. 4b (dotted line) at the position of the cross-peak Leu56 C$^{\delta2}$–H$^{\delta2}$. The full widths at half maximum (FWHM) are 90 Hz (solid line) and 140 Hz (dotted line). For easy comparison the traces were scaled to the same peak height.

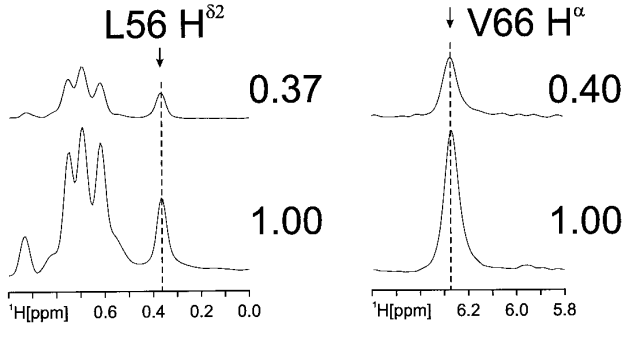

FIG. 6. 1D rows extracted from the spectra of Fig. 4a (upper traces) and Fig. 4b (lower traces) at the position of the cross-peaks Leu56 C$^{\delta2}$–H$^{\delta2}$ (see arrow in Fig. 4) and Val66 C$^{\alpha}$–H$^{\alpha}$ (not displayed in Fig. 4). To the right of the traces the normalized *S*/*N* ratios of the cross-peaks are given.

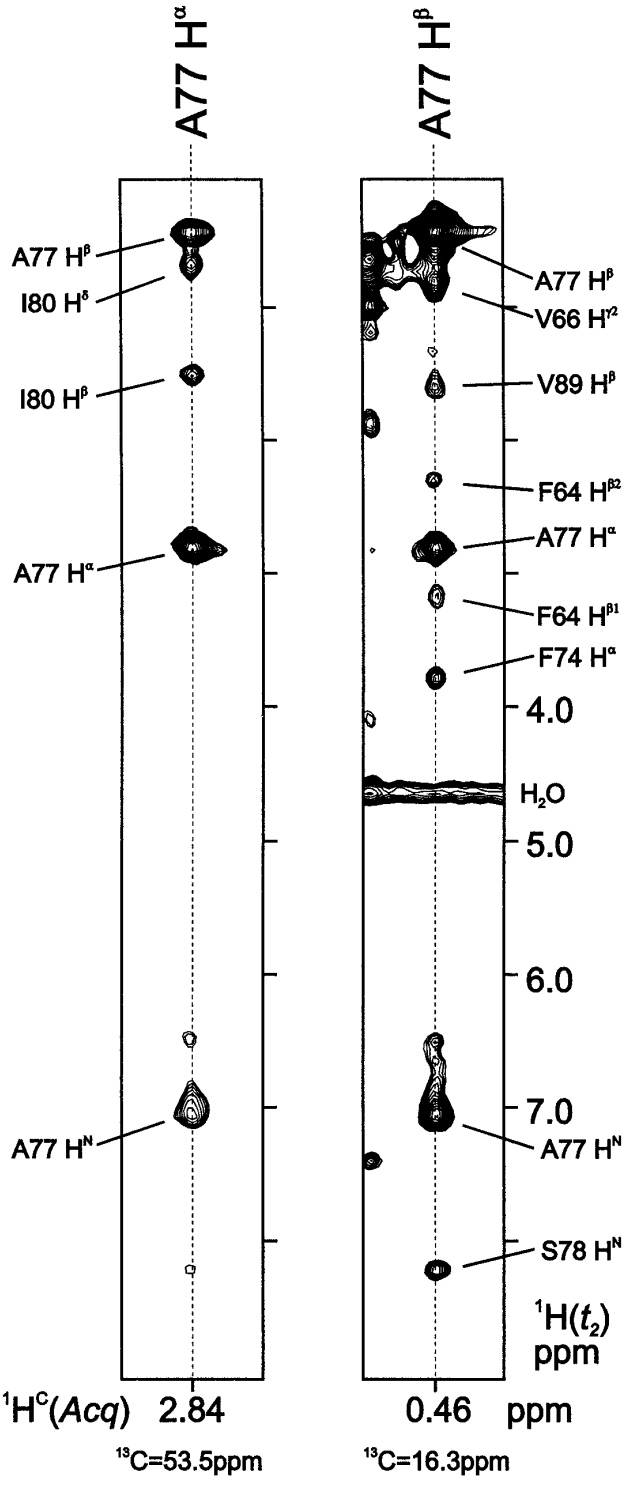

FIG. 7. Sample NOE traces (Ala77 H^{α} and Ala77 H^{β}) taken from the high-resolution ^{13}C-NOESY-HSQC spectrum of IIA^{Man} (Fig. 1b). The NOESY experiment was recorded over 3 days with a total size of 160 × 224 × 1024 real points (domains $^{13}C(t_1) \times {}^{1}H(t_2) \times {}^{1}H^{C}(Acq)$) with spectral widths of 5000 Hz × 7143 Hz × 8333 Hz. The ^{13}C domain was folded. The recording followed the protocol given in the legend of Fig. 1, but only two scans (first block) and eight scans (second block) repeating the first two steps of the phase cycle were accumulated. Therefore, the axial artifacts at the position of the ^{13}C source frequency did not cancel out. However, since the ^{13}C source frequency was set to 40.4 ppm, these artifacts appear in a sparsely populated region of the spectrum. The amplitude of the FIDs from the second $^{13}C(t_1)$-block were divided by 2 and the FIDs were resorted to remove interleaving of $^{13}C(t_1)$ and $^{1}H(t_2)$ data before processing. The data was processed to a matrix of 256 × 256 × 512 real points after apodization with a 90° shifted sine-bell window function and subsequent zero filling in all dimensions.

^{13}C) couplings (cosine-shaped decay) was chosen as the maximal evolution time in the two periods d' and d for all further experiments. This choice ensures a good combination of resolution and intensity in the case of the IIA^{Man} sample.

To investigate signal intensity and resolution of the experiments, the ^{13}C-HSQC experiment (Fig. 1a, 8-ms evolution time in both carbon evolution periods, measurement time 46 min) and a standard ^{13}C-HSQC (*20*) (8 ms carbon evolution time, measurement time 46 min) were recorded on the IIA^{Man} sample. Figure 4 shows details from the methyl region of both spectra. Obviously, the carbon linewidths in the plot of the new experiment (a) are significantly reduced, leading to the separation of some previously unresolved cross-peaks, such as Leu17 $C^{\delta 2}$–$H^{\delta 2}$ and Leu114 $C^{\delta 2}$–$H^{\delta 2}$. For a representative cross-peak (Leu56 $C^{\delta 2}H^{\delta 2}$) the full width at half maximum (FWHM) is reduced by 36% to 90 Hz (Fig. 5). This also shows that the resolution of the new experiment is still below the actual linewidth of most IIA^{Man} carbons (ca. 30 Hz, as determined from a ^{13}C-HSQC spectrum with a long carbon evolution time), ruling out wasteful overdigitization. To compare the sensitivity of the two experiments, 1D rows containing representative signals were extracted from either spectrum (Fig. 6). These signals show a reduction in *S*/*N* to about 40% for the new high-resolution experiment. The reduction stems in part from the handling of the two evolution periods using the ^{13}C–^{13}C gradient echo (*11*). However, the biggest loss is due to recording more of the very weak signal at the end of the rapidly decaying FID ($T_2 \approx 8$ ms for a typical C^{α} of IIA^{Man}).

The high-resolution 3D ^{13}C-NOESY-HSQC experiment (Fig. 1b) was recorded on the IIA^{Man} sample with the same value of 8 ms for the maximal evolution time in the two carbon evolution periods. The experiment was recorded over 3 days. The traces shown in Fig. 7 demonstrate the good sensitivity of the experiment in the case of large proteins, as even weak cross-peaks can be easily observed (e.g., all $C^{\alpha}(i)$–$H^{\alpha}(i)$–$H^{N}(i)$ cross-peaks were observed). Figure 8 shows a $^{1}H(t_2)$–$^{13}C(t_1)$ cross-section extracted at a chemical shift of 0.69 ppm in the acquisition domain $^{1}H^{C}(Acq)$. The NOE traces of resonances Leu17 $H^{\delta 2}$ and Leu114 $H^{\delta 2}$ are largely separated, and additional NOE restraints were obtained.

CONCLUSION

We describe a ^{13}C-HSQC experiment and the derived ^{13}C-NOESY-HSQC experiment with two separated periods for

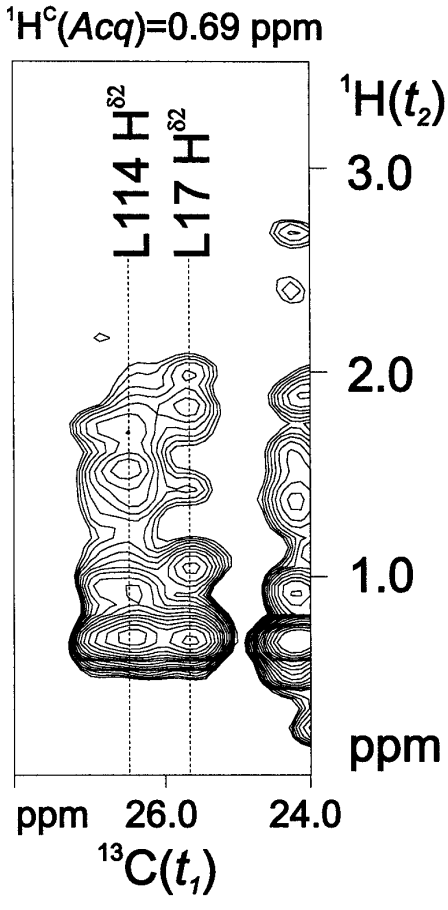

FIG. 8. $^1H(t_2)$–$^{13}C(t_1)$ cross-section of the high-resolution ^{13}C-NOESY-HSQC spectrum of the IIA^{Man} protein containing the traces of Leu114 $H^{\delta 2}$ and Leu17 $H^{\delta 2}$.

carbon evolution. The use of the two periods, each of which is kept below the time required for significant ^{13}C–^{13}C *J*-coupling, renders all ^{13}C homonuclear *J*-couplings ineffective. The information from the two periods is combined to a data set corresponding to evolution over the added duration of both periods via a ^{13}C–^{13}C gradient echo. For large proteins the sensitivity of the ^{13}C-HSQC experiment is lower than that of a standard ^{13}C-HSQC experiment, but far better than that of the constant time version with an evolution time of 28 ms. Applied to the 31-kDa IIA^{Man} protein, the linewidths observed in the ^{13}C-HSQC spectrum recorded in two blocks of 8 ms carbon evolution time each are reduced by about 36% compared to the standard ^{13}C-HSQC experiment, while the *S*/*N* of representative cross-peaks is lowered to about 40%. A ^{13}C-NOESY-HSQC experiment based on this ^{13}C-HSQC experiment has enabled us to evaluate additional NOE distances between resonances which were previously unresolved.

ACKNOWLEDGMENTS

This work was supported by the Deutsche Forschungsgemeinschaft and the Fonds der Chemischen Industrie. We thank Dr. Ralf Peteranderl (Technische Universität München) for thorough reading of the manuscript and valuable discussions.

REFERENCES

1. J. Jeener, B. H. Meier, P. Bachmann, and R. R. Ernst, *J. Chem. Phys.* **71,** 4546–4553 (1979).
2. A. Kumar, R. R. Ernst, and K. Wüthrich, *Biochem. Biophys. Res. Commun.* **95,** 1 (1980).
3. K. Wüthrich, ''NMR of Proteins and Nucleic Acids,'' pp. 117–130. Wiley, New York (1986).
4. S. W. Fesik and E. R. P. Zuiderweg, *J. Magn. Reson.* **78,** 588–593 (1988).
5. L. E. Kay, G. M. Clore, A. Bax, and A. M. Gronenborn, *Science* **249,** 411–415 (1990).
6. D. R. Muhandiram, N. A. Farrow, G.-Y. Xu, S. H. Smallcombe, and L. E. Kay, *J. Magn. Reson. B* **102,** 317–321 (1993).
7. G. W. Vuister and A. Bax, *J. Magn. Reson.* **98,** 428–435 (1992).
8. K. Hallenga and G. M. Lippens, *J. Biomol. NMR* **5,** 59–66 (1995).
9. M. Sattler and S. W. Fesik, *Structure* **4,** 1245–1249 (1996).
10. D. Nietlispach, R. T. Clowes, R. W. Broadhurst, Y. Ito, J. Keeler, M. Kelly, J. Ashurst, H. Oschkinat, P. J. Domaille, and E. D. Laue, *J. Am. Chem. Soc.* **118,** 407–415 (1996).
11. M. Baur and H. Kessler, *J. Magn. Reson.* **126,** 270–273 (1997).
12. A. Bax and S. Pochapsky, *J. Magn. Reson.* **99,** 638–643 (1992).
13. A. L. Davis, J. Keeler, E. D. Laue, and D. Moskau, *J. Magn. Reson.* **98,** 207–216 (1992).
14. J. E. Tanner, *J. Chem. Phys.* **52,** 2523–2530 (1970).
15. J. Stonehouse, P. Adell, J. Keeler, and A. J. Shaka, *J. Am. Chem. Soc.* **116,** 6037–6038 (1994).
16. T. Parella, *Magn. Reson. Chem.* **34,** 329–347 (1996).
17. M. Baur and H. Kessler, *Magn. Reson. Chem.* **35,** 877–882 (1997).
18. B. Stolz, M. Huber, Z. Markovic-Housley, and B. Erni, *J. Biol. Chem.* **268,** 27094–27106 (1993).
19. S. Seip, J. Balbach, S. Behrens, H. Kessler, K. Flükiger, R. de Meyer, and B. Erni, *Biochemistry* **33,** 7174–7183 (1994).
20. C. Griesinger, H. Schwalbe, J. Schleucher, and M. Sattler, in ''Two-Dimensional NMR Spectroscopy'' (Eds. W. R. Croasmun, R. M. K. Carlson), pp. 457–580. VCH, Weinheim (1994).
21. D. J. States, R. A. Haberkorn, and D. J. Ruben, *J. Magn. Reson.* **48,** 286–292 (1982).
22. D. Marion, M. Ikura, R. Tschudin, and A. Bax, *J. Magn. Reson.* **85,** 393–399 (1989).
23. A. J. Shaka, P. B. Barker, and R. Freeman, *J. Magn. Reson.* **64,** 547–552 (1985).
24. A. J. Shaka, J. Keeler, and R. Freeman, *J. Magn. Reson.* **53,** 313–340 (1983).